Optical Processing of Microwave Signals - Part B

Jean Chazelas
Thales Airborne Systems
2 Avenue Gay Lussac,78851 Elancourt Cedex
Daniel Dolfi, Sylvie Tonda-Goldstein, Jean-Pierre Huignard, Thales Research & Technology
91401 Orsay Cedex, France

Abstract

The availability of optoelectronic components operating up to 20 GHz brings attractive perspectives for optical processing of microwave signals. Furthermore optically carried microwave signals can experience large time delays, especially in fiber based systems, providing time-frequency products in the range between 10^2-10^3. Owing to their inherent parallel processing capabilities, optoelectronic architectures are well suited for the implementation in radar and electronic warfare systems of basic functions such as spectrum and time delay analysis, adaptive and programmable filtering, correlation and waveform generation.
This document is prepared for the NATO's RTA Lecture Series 299 on Optics and Microwave Interactions to be presented in September 2002

1. Programmable transversal filtering- Thales approach

A transversal filter optimizes the detection in a signal $x(t) = S(t) + N(t)$ of a given signal S(t) with duration T, in presence of a stationary noise N(t) or permits jammers rejection from detected signals. These signals are often processed in a sampled form using digital electronic delay lines, allowing a rather large number of sampling points (up to 10^2 - 10^3), but with a frequency bandwidth limited to the low and intermediate frequencies (100 MHz-1 GHz). This frequency bandwidth can be extended up to the 10 GHz region using optoelectronic architectures, especially in fiber based systems, but with the limitation of a number of sampling points in the range 10-10^2.
Therefore, we propose a free space optical architecture of a programmable filter which could provide a large number of samples of about 10^3 and which may process signals over a frequency bandwidth as large as 20 GHz. The operating principle of this programmable filter is shown in figure 1.

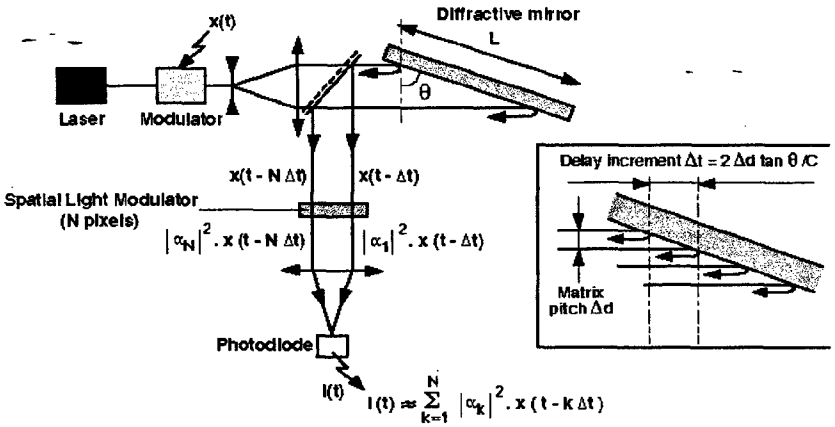

Figure1 Programmable transversal optical filter

Paper presented at the RTO SET Lecture Series on "Optics Microwave Interactions", held in Jouy en Josas, France, 2-3 September 2002; Duisburg, Germany, 5-6 September 2002; Budapest, Hungary, 9-10 September 2002, and published in RTO-EN-028.

A CW laser diode is coupled into an integrated optic amplitude modulator, excited by a microwave signal x(t). This provides an optical carrier of this signal x(t). This optical carrier is expanded and reflects off a diffractive mirror, which operates in the Littrow geometry and provides the necessary time delays. This reflected beam, extracted with a beam-splitter, passes through a one dimensional LCSLM of N pixels providing parallel weighting. Finally the channelized beam is focused onto a photodiode. The response time of the proposed programmable filter is mainly determined by the response time of the liquid crystal SLM (in the range 10-100 μs for ferroelectric or chiral smectic LC). In order to meet radar or EW systems requirements in term of adaptive processing speed in the range 10 ns - 10 μs, it would be necessary to use multiple quantum well SLMs or to take advantage of the high resolution of LCSLMs. Furthermore, it is possible to extend the concept to a 2D geometry including a photodiode array in order to provide high speed processing and large time delays, i.e time-frequency products up to 10^3-10^4.

As a proof of concept a simple rejection filter is implemented using a CW fiber laser (40 mW at 1550 nm). It is coupled to an integrated optic Mach-Zehnder modulator, excited by a CW microwave signal. An image of two slits is displayed onto the SLM, providing two out-of-phase signals. The diffractive mirror operates in the double pass geometry, providing a measured maximum delay of 750 ps. In these conditions, using a multimode-fiber pigtailed photodiode, it is possible to measure at 1.3 GHz a 52 dB signal rejection as shown in figure 2.

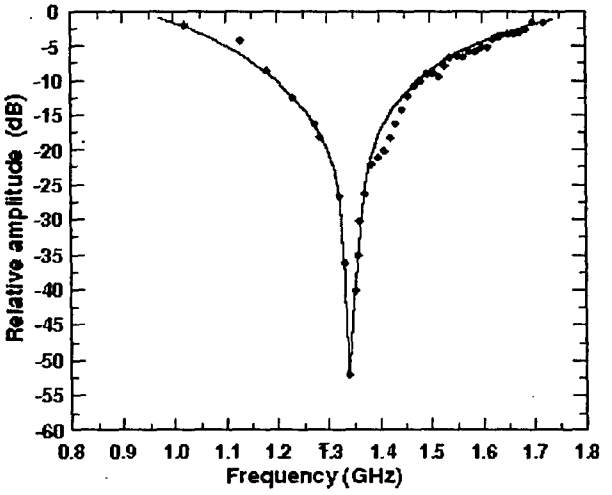

Figure 2 52 dB stop-band filter at 1.3 GHz

2. Optical waveform generation

In order to increase the resolution and the jamming robustness of radar systems, highly complex synthetic waveforms are needed to perform sophisticated signal processing functions at high speed. Typical nowadays solutions are based on digital processing techniques requiring high speed sampling of the signals. Hundreds of thousands sampling points with 8 to 10 bits coding are required because the radar pulse typically lasts 1 to 10μs for radar frequency of 10GHz in 1GHz-bandwidth. A new realistic solution would be to exploit and combine the flexible numerical processing strengths of electronics with the communication and parallel processing strengths of optics to accomplish computationally intensive tasks with

high processing speed. We propose and demonstrate an arbitrary waveform generator based on the heterodyne detection of optically carried microwave signals whose phase and amplitude is optically controlled through the use of LCSLMs.
The operating principle of controlling the amplitudes and phases of optical carriers of microwave signals using heterodyne detection is depicted in Figure 3. It is based on a combination of the basic principles already illustrated in the previous applications. A single-frequency laser beam (ω) is focused through an anisotropic acousto-optic Bragg cell (BC), excited by a continuous microwave signal at pulsation 2πf.

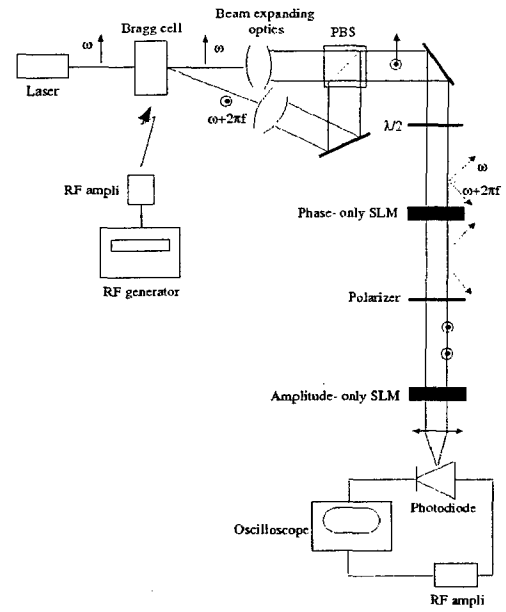

Figure 3:Experimental set-up of the control of amplitudes and phase of optically carried microwave signals.

The transmitted beam (ω) and the diffracted beam (ω+2πf) at the output of the Bragg cell are cross-polarized. They are recombined without loss on a polarizing beam splitter (PBS) to get a dual-frequency optical carrier for the microwave signal. When a photodiode detects this dual-frequency beam through a 45°-oriented polarizer, a microwave beating signal at frequency f is observed. The dual-frequency beam intercepts a first nematic liquid crystal (NLC) spatial light modulator (SLM1) of P pixels providing P channelized beams. This phase-only SLM permits, independently on each channel, an analog phase control of the optically carried microwave signal by changing the relative optical phase of the cross-polarized components of the dual-frequency beam. Next, a twisted nematic liquid crystal (TNLC) SLM (SLM2) of P pixels, placed between two crossed polarizers (polarizing beam splitter PBS at input and exit polarizer at output of SLM2), provides the amplitude control of the microwave signals. Images up to 8 to 10 bits are displayed on the TNLC cell, so that the transmission of each pixel of SLM2 is changed. By control of the displayed grey levels onto the TNLC cell, the amount of light passing through the exit polarizer is controlled, giving an amplitude-controlled output microwave signals. At the output of SLM2, the beating signal is detected at the photodiode. According to the set-up features (photodiode area, optical wavelength, number and size of the SLM pixels and focal length), the amplitudes of the optical signals are coherently summed onto the photodiode, thus also generating coherent summation in the electrical domain of the optically carried microwave signals.

For microwave signals composed of several frequencies, as it is the case for radar pulses, the acousto-optic Bragg cell has to be excited by several continuous microwave signals at different frequencies f_k, (k=1 to N). Each diffracted beam, frequency-shifted by f_k passes through one given pixel i (i=1 to P) of the SLMs'. We control independently the features of each microwave frequency component f_k (phase and amplitude) by the control of the transmission law of the SLMs'. When attributing one frequency to a given pixel i and when doing so for all the frequencies of a given radar spectrum, one can generate any arbitrary waveform. In practical case, a radar antenna transmits a coherent pulse train e(t) that has a pulsewidth T and an interpulse period PRI=1/PRF. The Fourier transform of the pulse train has a sinc(u) envelope, modulating a series of spectral lines f_k spaced by the PRF of the radar ($f_k=f_a+kPRF$, k=-∞..+∞). The peak of this response is at the radar center frequency f_a, and the zeros of the sinc(u) envelope are located at frequencies $f_a \pm j/T$ (j=-∞..+∞) where T is the pulse width. At the output of the SLMs', and on channel i, the expression of the modulated microwave signal is :

$$s(t) = \frac{1}{2}\sum_{k=0}^{+\infty} a_{k,i} E_k \left(\cos(2\pi f_{k,i} t + \phi_{k,i}) + \cos(2\pi f_{-k,i} t + \phi_{-k,i})\right)$$

where the coefficients $a_{k,i}$ are the attenuations of the frequencies $f_{k,i}$ due to the pixel i of the amplitude-only SLM2 and $\Phi_{k,i}$ the phase shifts introduced by the pixel i of the phase-only SLM1. The E_k coefficients are the Fourier coefficients of the coherent pulse train. The frequency $f_{k,i}$ is associated to the pixel i and $f_{-k}=f_a-kPRF$ and $f_{+k}=f_a+kPRF$. We decompose the output signal s(t) onto the kPRF frequencies of the envelope in order to be able to modify s(t) by arbitrary changing the parameters (a_k,Φ_{+k} and Φ_{-k}).

According to the Fourier Transform of the radar pulse train, two consecutive frequencies f_k and f_{k+1} are spaced from only PRF=1/PRI, that is in the range of a few tens of kHz. In order to cope with this low resolution, we propose an alternative optical architecture (Figure 7) that combines an acousto-optic Bragg cell (BC) with a moving grating that diffracts multiple orders. The moving enforced to the grating is driven by applying a periodical signal on the grating. We consider as for the frequency of the applied signal, the frequency of the radar pulse train: f_s=PRF.

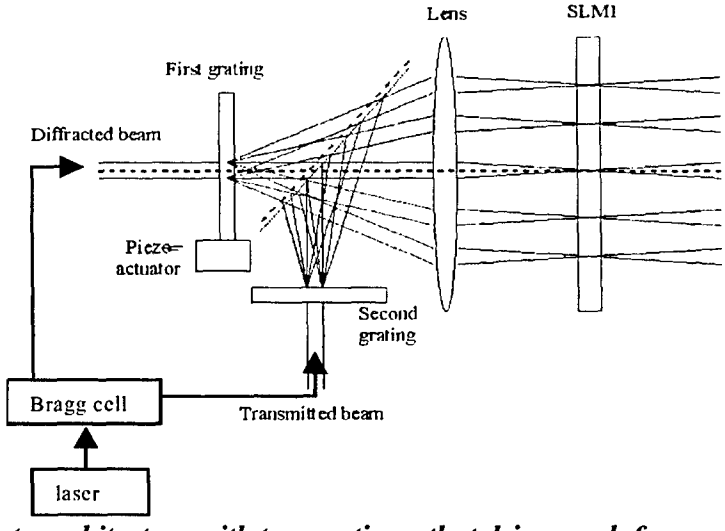

Figure 4: kHz rate architecture with two gratings, that drives each frequency component at kPRF towards each pixel.

In order to modulate the maximum number of frequencies, the grating should diffract many orders. The second grating in the Figure 4 is a fixed one that diffracts the transmitted beam coming from BC. This architecture has the advantage to discriminate the optical beams on the

assumption of SLMs' with classical sizes of pitches (larger than 40µm). According to the required kHz frequency shift, the Raman-Nath grating (first grating) is moved using a piezoelectric actuator, excited with a sawtooth signal of pulsation $2\pi f_s$. This moving grating creates a Doppler shift resulting in diffracted orders at pulsation $\omega+2\pi kf_s$. Owing to the capabilities of the Bragg cell combined with the moving grating, the optical architecture enables us to drive each frequency f_k shifted by kPRF towards each pixel i of the SLMs'. The microwave carrier f_a and the frequency spectrum of the radar f_s are respectively transposed on the optical carrier by the Bragg cell and the moving grating. Figure 5 presents the complete optical architecture of the proposed arbitrary waveform generator.

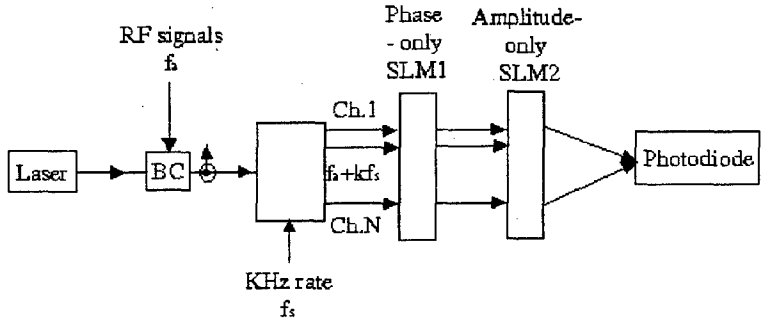

Figure 5: Complete optical architecture of the proposed arbitrary waveform generator

A proof of concept is experimentally demonstrated using two computer-controlled SLMs of 4x4 pixels. Each pixel is 3.5x3.5mm^2 and exhibits an optical transmission of 95%. It permits to explore amplitude and phase ranges of 30dB and 2π rad respectively. The Bragg cell central frequency is 2GHz with bandwidth of 2GHz. Our aim was to control independently the features of the two frequencies (phase and amplitude). We used two RF generators and a combiner to sum the two RF signals. Owing to an appropriate set-up, the two diffracted beams at the output of the Bragg cell were made to travel in parallel through two different pixels of the 4x4 pixel SLM. The signal detected at the photodiode was composed of a carrier at frequency $(f_1+f_2)/2$ and an envelope at frequency $(f_1-f_2)/2$. By switching off independently pixel 1 or pixel 2 of the amplitude-only SLM, we were able to attenuate of 25dB either the spectrum line 1 or the spectrum line 2 of a dual-frequency signal (Δf=45MHz).
We also demonstrated the control of a pulse train (pulsewidth T=12ns and interpulse period PRI=77ns, PRF=13MHz). Because the pixel sizes of the SLM we used were quite large (3.5x3.5mm^2), the signal modulation could only be realized with two pixels. Figure 9 shows the sinc(u) envelope when the light beams travel through the two pixels. The spectrum lines are spaced of 13MHz. We first verified that switching off all the pixels causes all the spectrum lines to disappear (top of Figure 6), next, that switching off one pixel causes a part of the spectrum to disappear (bottom of Figure 6). For example, the extinction of pixel 1 leads to the attenuation of the left lines with respect to the central line. And the extinction of pixel 2 leads to the attenuation of the right lines. The attenuation of the lines was about 25dB, which is close to the SLM maximum attenuation.

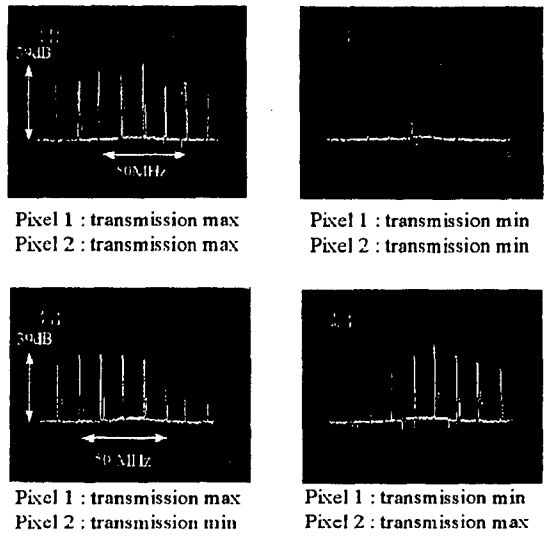

Figure 6: Amplitude modulation in case of a pulse train (T=12ns, PRI=77ns).

We have finally demonstrated with the experimental set-up of Figure 5 that the moving grating controlled by a piezoelectric material permits us to increase the resolution of the architecture. A 1µm-step grating was used that combine the transmitted zero-order beam with the 1-order and 2-order beams. The periodic electrical signal was at 10kHz. The beating signals were detected at frequencies 10kHz for the 1-order beam and 20kHz for the 2-order beam.

3. Spectrum analysis and correlation

Acousto-optic spectrum analyser

The operating principle of an acousto-optic spectrum analyser is presented on figure 10

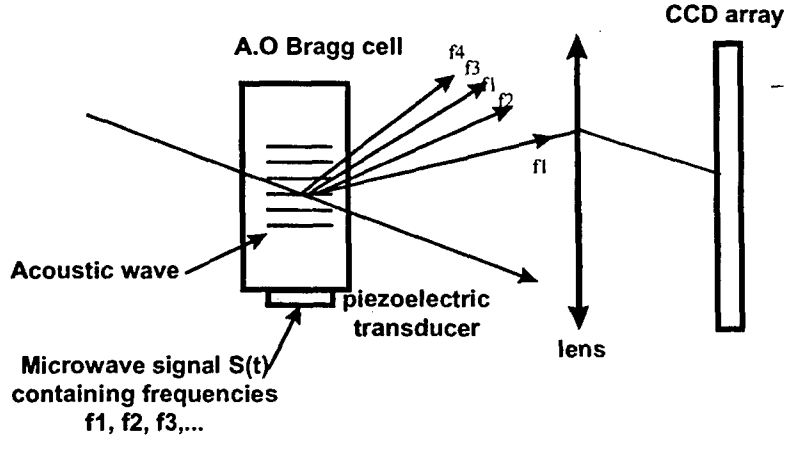

Figure 8.10 - Acousto-optic spectrum analyser

The microwave signal to be analysed is applied onto a piezoelectric transducer, glued on an elasto-optic material. In such a material, the refractive index is changed according to the locally applied pressure. Through the piezo-transducer a pressure wave (i.e an acoustic wave) is generated . It results in a travelling refractive index grating. Since this mechanism is a linear one, each frequency contained in the applied signal S(t) will results in a corresponding grating with a period $\Lambda_i=v/f_i$ (where v is the speed of the acoustic wave). In fact, each diffractive grating is a "frozen image" of the microwave signal. When a collimated laser beam travels through these superposed gratings, each grating will diffract the light in a given direction corresponding to the period Λ_i, with an efficiency proportional to power of frequency f_i. Those diffracted beams are then collected and "Fourier transformed" through the use of an optical lens on a CCD array. An image of the microwave spectrum is then displayed onto the CCD.

Typical performances of such systems are shown in the following list:

- central frequency F: typ. 1 to 2 GHz (up to 9 GHz, University Saratov)
  - mainly limited by the piezo transducer thickness (typ. few µm) and the acoustic absorption
- frequency bandwidth DF: 0.5 to 1 GHz (up to 3 GHz)
  - mainly limited by the acousto-optic/Bragg conditions
- frequency resolution : 1 to 3 MHz
  - linked to the central frequency and the time.frequency product
- diffraction efficiency: typ. 10% / W RF
  - maximum microwave power mainly limited by the piezo transducer thickness
- linear dynamic range: typ. 30 - 40 dB
  - mainly limited by the CCD array (acoustic linear dynamic range typ. 70 dB)

One of the main interest of the acousto-optic spectrum analysis was its wide instantaneous bandwidth and its low power consumption. Now a day, purely digital spectrum analysis can bring quite the same performances, taking advantage in addition of an extended compatibility with other digital processing functions.
According to the dynamic range limitation and the long access time (about 100 µs, linked to CCD response time and to the necessary propagation of the acoustic wave in the crystal) practical use of acouto-optic microwave spectrum anlyser is limited to radioastronomy (both ground based and spaceborne).

Frequency filtering

The combination of acousto-optic components with spatial light modulators permits the implementation of processing functions such as adaptive frequency filtering. The operating principle of such an architecture is shown on figure 11.

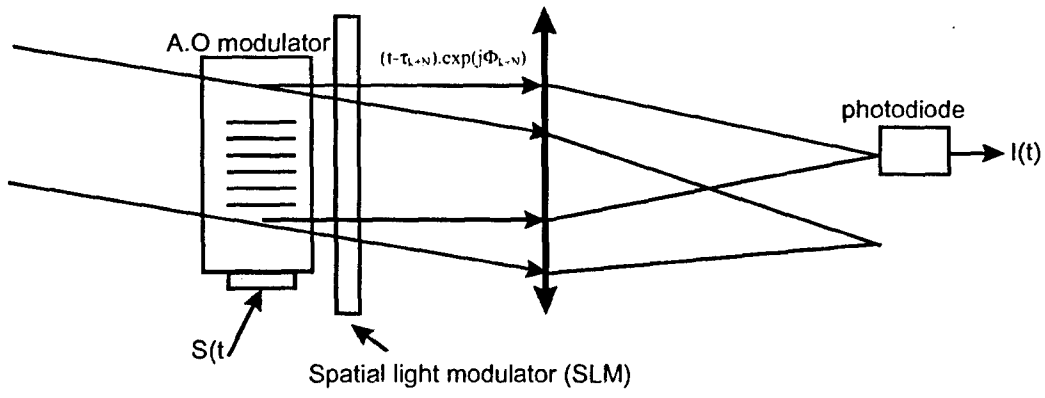

Figure 8.11 - Adaptive frequency filtering architecture

According to the spatial resolution of the SLM, this last one is arranged close to the Bragg cell or in the Fourier plane of the lens. Considering resolutions of about 100x100 pixels (obtained for example with liquid crystal SLMs), most of the experimental demonstrations were performed with the « SLM close to the Bragg cell » architecture.

The collimated laser beam diffracts off an acoustic replica of the electrical signal S(t) applied on the piezoelectric transducer. According to the propagation of the acoustic wave, each portion of the laser beam, along the acoustic column, will diffract with an efficiency proportional to the amplitude of the sample $S(t-\tau_i)$. Through the use of the SLM, it is possible to control the phase of the optical carrier of the microwave signal, for each sample. These sample are then coherently summed onto a high speed photodiode.
Considering the capability offered by 2D SLMs to provide reconfigurable complex phase law, sophisticated programmable filters can be performed with this type of architecture.
Typical parameters of experimental demonstrations of adaptive filtering are listed below :

- central frequency: 140 MHz
- max. duration of the signal: 2 µs
- frequency bandwidth: 90 MHz
- 256 pixels SLMs with phase delays up to 7π

Main limitations of this approach are :

- central frequency of about few hundreds MHz. In order to use high efficiency A .O Bragg cells, providing in addition acoustic column lengths corresponding to time of propagation of about few µs, it is necessary to operate with frequency lower than 300 MHz

– response time of liquid crystal SLMs of few tenth of milliseconds. It corresponds to the time of reconfiguration of the filter.

With this kind of performances, once again, now a day corresponding digital architectures offer better and more exploitable performances. But an increase of the operating frequency up to 1 GHz (potentially possible with low loss materials) combined for instance with SLMs response as low as 0.1µs would provide performances largely exceeding those of numerical filters.

Acousto-optic correlators

The operating principle is described on figure 12

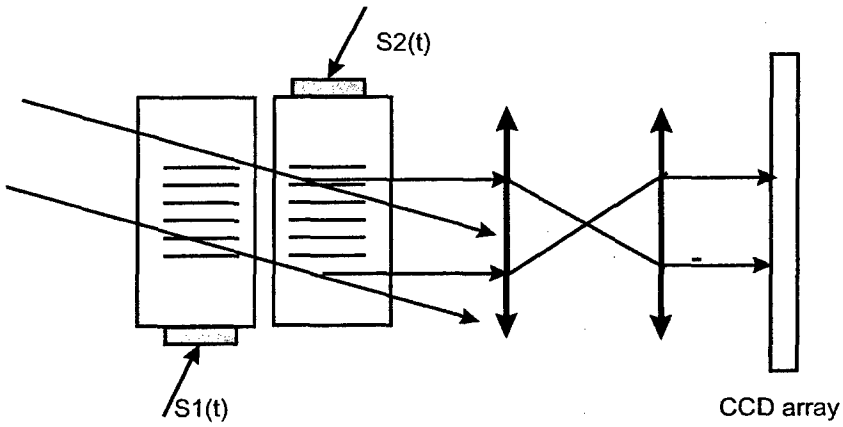

Figure 8.12 - Acousto-optic correlator principle

The microwave signals $S_1(t)$ and $S_2(t)$ are respectively applied on two acousto-optic Bragg cells, in which the acoustic wave propagate in opposite directions. In this case, on each pixel of the CCD, the detected, and potentially integrated, amount of light will be propotional to $S_1(t).S_2(t-\tau_i)$.

Another way to implement the same function would be to use the following architecture.

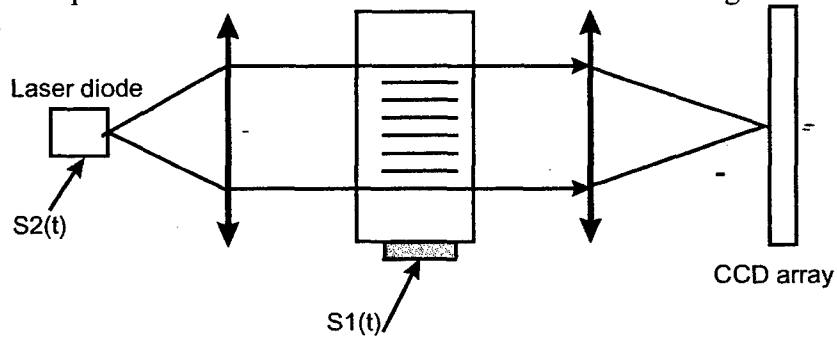

In this case the first A.O cell is replaced by a modulated (directly or externally) laser source which is fed with signal $S_1(t)$.

In both cases the correlation function of the two signals appear as a spatially varying function along the CCD array.

Main advantage of this type of correlator is to permit the analysis of long microwave pulses (up to few hundreds of milliseconds). Most of the practical implementations are thus devoted to radioastronomy applications with the following typical performances :

- central frequency: 100 MHz
- frequency bandwidth: 10 MHz
- time of integration : 10 ms

Time of integration up to 100 ms - 1s (corresponding to time.frequency products and compression coefficients of 10^6 = 10 MHz x 100 ms) can be obtained through the association of a CCD array with a digital memory.

4. REFERENCES

1. D. Norton, S. Johns, C. Keefer and R. Soref, "Tunable microwave filtering using high dispersion fiber time delays", *IEEE Photon. Tech. Lett.*, vol 6, pp. 831-832, 1994.
2. M.Y. Frankel and R.D. Esman, "Fiber-optic tunable transversal filter", *IEEE Photon. Tech. Lett.*, vol 7, pp. 191-193, 1995.
3. D. Dolfi et al, "Optical architectures for programmable filtering and correlation of microwave signals", *IEEE Trans microwave Theory Tech.* Vol 45, pp. 1467-1472, 1997.
4. .P. Foord, P.A. Davies and P.A. Greenhalgh, "Synthesis of microwave and millimetre-wave filters using optical spectrum-slicing", *Electron. Lett.*, vol 32, pp. 390-391, 1996.
5. J. Capmany, D. Pastor and B. Ortega, "Fibre-optic microwave and millimetre wave filter with high density sampling and very high sidelobe supression using subnanometre optical spectrum slicing", *Electronics Letters,* 1999, pp. 494-496.
6. J. Capmany, J. Cascón, D. Pastor y B. Ortega, "Reconfigurable fiber-optic delay line filters incorporating electrooptic and electroabsorption modulators", *IEEE Photonics Technology Letters*, 1999, pp. 1174-1176
7. G.A. Ball, W.H. Glenn and W.W. Morey, "Programmable fiber optic delay line", *IEEE Photon. Technol. Lett.*, vol 6, pp. 741-743, 1994.
8. Molony, C. Edge and I. Bennion, "Fibre grating time delay for phased array antennas", *Electron. Lett.*, vol 31, pp. 1485-1486, 1995.
9. D.B. Hunter and R.A. Minasian, "Reflectivity tapped fibre-optic transversal filter using in-fibre Bragg gratings", *Electron Lett.*, vol 31, pp. 1010-1012, 1995.
10. D.B. Hunter and R.A. Minasian, "Tunable transversal filter based on chirped gratings", *Electron. Lett.*, vol 31, pp. 2205-2207, 1995.
11. D.B. Hunter and R.A. Minasian, "Microwave optical filters using in-fiber Bragg grating arrays", *IEEE Microwave and Guided Wave Lett.*, vol 6, pp. 103-105, 1996.
12. D.B. Hunter and R.A. Minasian, "Photonic signal processing of microwave signals using active-fiber Bragg-grating-pair structure", *IEEE Trans. Microwave Theory and Techn*, vol 8, pp. 1463-1466, 1997.
13. J.L. Cruz, B. Ortega, M.V. Andres, B. Gimeno, D. Pastor, J. Capmany and L. Dong, "Chirped fibre Bragg gratings for phased array antennas", *Electron. Lett.*, vol 33, pp. 545-546, 1997.
14. D.B. Hunter and R.A. Minasian, "Microwave optical filters based on fibre Bragg grating in a loop structure", *Proc OFC '97*, paper TH2-2, pp. 273-275.
15. D.B. Hunter and R.A. Minasian, "Microwave optical filters based on fibre Bragg grating in a loop structure", *Proc OFC '97*, paper TH2-2, pp. 273-275.

16. D.B. Hunter and R.A. Minasian, "Photonic signal processing of microwave signals using active-fiber Bragg-grating-pair structure", *IEEE Trans. Microwave Theory and Techn*, vol 8, pp. 1463-1466, 1997.
17. S.C. Kim, et al, "Recirculating fiber delay line filter using a fiber Bragg grating", *IEEE LEOS '98 Digest.*, pp. 328-329, 1998.
18. D. Pastor and J. Capmany, "Fiber optic tunable transversal filter using laser array and linearly chirped fibre grating", *Electronics Letters*, 1998, pp. 1684-1685.
19. J. Capmany, D. Pastor and B. Ortega, "Experimental demonstration of tunability and transfer function reconfiguration in fibre-optic microwave filters composed of a linearly chirped fibre grating fed by a laser array", *Electronics Letters*, 1998, pp.2262-2264
20. W. Zhang, J.A.R. Williams, L.A. Everall and I. Bennion, "Fibre-optic radio frequency notch filter with linear and continous tuning by using a chirped fibre grating", *Electron. Lett.*, vol 34, pp. 1770-1772.
21. W. Zhang, J.A.R. Williams, L.A. Everall and I. Bennion, "Tuneable radio frequency filtering using linearly chirped fibre grating", *proc ECOC '98*, pp. 611-612, 1998.
22. D.B. Hunter and R.A. Minasian, "Tunable microwave fiber-optic bandpass filters", *IEEE Photon. Technol. Lett*, vol 11, pp. 874-876, 1999.
23. N. You and R.A. Minasian, "Synthesis of WDM grating based optical microwave filter with arbitrary impulse respose", *Int. Top. Meeting MWP '99 Digest*, pp. 223-226, 1999.
24. N. You and R.A. Minasian, "A novel high-Q optical microwave processor using hybrid delay line filters", *IEEE Trans. Microwave Theory Tech.*, vol 47, pp. 1304-1308, 1999.
25. R. Minasian, "Photonic signal processing of high speed signals using fiber gratings", *Int. Top. Meeting MWP '99 Digest*, pp. 219-223, 1999.
26. W. Zhang, J.A.R. Williams, L.A. Everall and I. Bennion, "Tuneable radio frequency filtering using linearly chirped fibre grating", *proc ECOC '98*, pp. 611-612, 1998.
27. K.J. Williams, J.L. Dexter and R.D. Esman, "Photonic microwave signal processing", *Int. Top. Meeting MWP '98 Digest*, pp. 187-189. 1998.
28. W. Zhang, J.A.R. Williams and I. Bennion, "Recirculating fiber-optic notch filter employing fiber gratings", *IEEE Photon. Technol. Lett.*, vol 11, pp. 836-838, 1999.
29. J. Capmany, D. Pastor and B. Ortega, "Efficient sidelobe supression by source power apodisation on fibre-optic microwave filters composed of linearly chirped fibre grating fed by laser array", *Electronics Letters*, 1999, pp. 640-642.
30. J. Capmany, D. Pastor, B. Ortega, "Applications of fibre Bragg Gratings to Microwave Photonics", *IEE Colloquium on fibre gratings 1999*, Birmingham, UK.
31. J. Capmany, D. Pastor and B. Ortega, "New and flexible fiber-optic delay line filters using chirped Bragg gratings and laser arrays", *IEEE Trans. Microwave Theory Tech.*, vol 47, pp. 1321-1327, 1999.
32. P.J. Mathews and P.D. Biernacki, "Photonic signal processing for microwave applications", *IEEE MTT-S Digest*, paper WE1B-1, pp. 877-880, 1999.
33. D. Pastor, J. Capmany and B. Ortega, "Experimental demonstration of parallel fiber-optic-based RF filtering using WDM technique", *IEEE Photonics Technology Letters*, 2000, pp. 77-79.
34. R.A. Minasian, "Photonic signal processing of high-speed signals using fiber gratings", *Opt. Fib. Tech.*, vol 6, pp. 91-108, 2000.
35. W. Zhang, J.A.R. Williams and I. Bennion, "Optical fibre delay line filter free of limitation imposed by optical coherence", *Electron.Lett.*, vol 35, pp. 2133-2134, 1999.
36. Ho-Quoc, S. Tedjini and A. Hilt, "Optical polarization effect in discrete time fiber-optic structures for microwave signal processing", *IEEE MTT- Symposium Digest*, pp. 907-910, 1996.

37. F. Coppinger, S. Yegnanarayanan, P.D. Trinh and B. Jalali, "All-optical incoherent negative taps for photonic signal processing", *Electron. Lett.*, vol 33, pp. 973-975, 1995.
38. M. Tur and B. Moslehi, "Laser phase noise effects in fiber-optic signal processors with recirculating loops", *Opt. Lett.*, vol 8, pp. 229-231, 1983.
39. M. Tue, B. Moslehi and J.W. Goodman, "Theory of laser phase noise in recirculating fiber optic delay lines", *IEEE J. Lightwave Technol*, vol 3, pp. 20-30, 1985.
40. M. Tur and A.Arie, "Phase induced intensity noise in concatenated fiber-optic delay lines", *IEEE J. Lightwave Technol.*, vol 6, pp. 120-130, 1988.
41. B. Moslehi, "Analysis of optical phase noise in fiber-optic systems employing a laser source with arbitrary coherence time", *IEEE J. Lightwave Technol.*, vol 4, pp. 1334-1351, 1986.
42. J.T. Kringlebotn and K. Blotekjaer, "Noise analysis of an amplified fiber-optic recirculating delay line", *IEEE J. Lightwave Tech*